

# Applied Master Lab Course: Diamonds for Sensing Applications

J.-P. Schröder, D. Palani, O. Orlov, T. Schaetz, and U. Warring

*Albert-Ludwigs-Universität Freiburg, Physikalisches Institut,*

*Hermann-Herder-Straße 3, 79104 Freiburg, Germany*

(Dated: April 4, 2018)

Diamonds inhabit a variety of color centres, one of particular interest is the so-called nitrogen-vacancy (NV) centre. It is studied in great detail in quantum physics research and it is a promising platform for sensing applications on a molecular level. The goals of this lab course is for the students to investigate the principles of magnetic field sensing with NV centres in diamonds. During the course they learn to apply/optimize laser light and microwave fields in the context of quantum physics experiments and to analyse spectral resonances.

*Keywords: Nano-diamonds, diamond lattice, NV centre, diode laser, microwaves, fluorescence spectroscopy, optically detected magnetic resonance, and Zeeman effect*

*Training skills: Optics and laser beam alignment, electronics, and data acquisition/analysis.*

## CONTENTS

I. Introduction	1
A. NV centres within the lattice structure	2
B. Quantum properties of NV centres and sensing applications	2
C. NV fluorescence and optically detected magnetic resonances	3
II. Experimental setup	4
A. Laser source and optical components	4
B. Electronic and microwave equipment	4
C. Apparatus for NV centre spectroscopy	4
III. Course program	5
A. Notes on performing measurements and data analysis	5
B. Calibration measurements	5
C. Compare the characteristics of multiple diamonds	5
IV. Appendix	6
References	6

## I. INTRODUCTION

Diamonds sparkle in a variety of colours and attract our attention for many different reasons. Besides their appeal as gemstones, they are known for their outstanding mechanical hardness, heat conductivity, electrical resistivity, chemical stability, and optical transparency. The natural occurrence in more than one distinct colour originates from so-called colour centres in diamonds. They are identified as fluorescent lattice defects, where carbon atoms are replaced by impurity atoms or vacant lattice sites. Each kind of defect is uniquely identifiable by its fluorescent/absorption spectrum. Today, we know more than several hundred distinct colour cen-

tres [1]. The physical properties of such defects in synthetic diamonds are studied, as they rise the promise for several different novel application within the fields of physics, nanotechnology, and life science [2–7]. For the latter, it is crucial that diamonds are judged non-toxic and, as such, they are well suited for bio-medical applications. They are heavily investigated in the context of, e.g., drug delivery and bio imaging [3]. A particular defect in diamonds has caught the attention of scientists during the last decades. It is comprised by a nitrogen atom and a neighbouring, vacant lattice site; the so-called nitrogen vacancy (NV) centre [5, 8]. In physics, its quantum mechanical properties are studied in detail, as those can be used for quantum information [2], simulation [6], and metrology [7] applications.

Notably, some of the employed methods and techniques for quantum control of the NV centres were developed in the field of nuclear magnetic resonance and atomic physics during the last century. These methodologies, e.g., enable high-precision measurements and control of the quantum degrees of freedom of individual atoms and are commonly applied for most accurate and precise atomic clocks and quantum information processing [9]. Unfortunately, quantum experiments require highest efforts in isolating individual, single atoms from their environment [10]. For example, ultra-high vacuum conditions and temperatures close to the absolute zero are essential and make versatile applications of atoms as sensors challenging. As the quantum nature (coherence) of NV centres is well protected by the surrounding diamond lattice, its sensor properties can be harnessed even under ambient conditions. NV centres are, therefore, ideal for sensing in rough environments, e.g., in aqueous solutions for life science applications. They have been demonstrated to be sensitive, e.g., to magnetic [11–13] and electric [14] fields, temperature [15], and pressure [16]. To use these defects as sensors, they are packed in small diamond crystallites of a few tens of nanometres in diameter [3, 5, 7] with about  $10^9$  carbon atoms. Recently, it has been demonstrated in a proof-of-principle experi-

ment that quantum measurements on nanodiamonds can be performed even inside living cells[? ]. However, to harness the full potential of such nanoscale sensors for metrology applications suitable techniques are required to control their spatial position and orientation, as well as, to efficiently manipulate their quantum state. Currently, several techniques are being investigated for spatial control [17–20], including optical tweezers and scanning probe approaches, in which nanodiamonds are attached, e.g., to atomic force microscope tips. In one of our lines of research, we investigate a novel approach to achieve that: We employ control and sensing methodologies that we previously demonstrated with individually trapped atomic ions and commonly use in the group of Prof. Schätz.

In this lab course, we study the spectral characteristics of NV centres in micro-sized diamonds. This includes measurements of their fluorescence spectra [5, 7] to identify different NV centres and recordings of optically detected magnetic resonances [5, 7] in the microwave regime. Finally, magnetic field sensing of neodymium (an alloy made of neodymium, iron, and boron) magnets placed in various spatial positions and orientations is employed to reconstruct the orientation of the mono crystalline lattice within the laboratory coordinate system. All of which are prerequisites for quantum state control of single NV centres for sensing applications.

### A. NV centres within the lattice structure

A nitrogen vacancy centre in the diamond lattice is comprised by a nitrogen atom replacing a carbon atom and an adjacent vacant lattice site. The spatial characteristics of the centre, i.e., its symmetries and other environmental conditions, tune the associated electronic state configurations, cp. Sec. I.B. The density of NV centres within (natural and synthetic) diamonds strongly depends on the conditions under which they are formed [5] and can even vary within individual diamonds that have been produced under the same conditions. Most efficiently, these centres are introduced in type-1b synthetic diamond samples through electron irradiation with energies of approx. 2 MeV and annealing at 600 K under vacuum conditions [5]. In this lab course we are using commercially mono crystalline powders (MSYmicron-diamond powder from Microdiamant AG) with different sized diamonds in the range of 25 nm up to 25  $\mu$ m. In these samples the NV density has not been intentionally increased during formation as they are typically used for diamond tools. In general, the symmetry axis of the NV centres can (only) be aligned along the crystallographic directions and Fig. 1 depicts possible orientations with the face-centred cubic Bravais lattice. Typically, the eight possible orientations are labelled according to corresponding Miller indices.

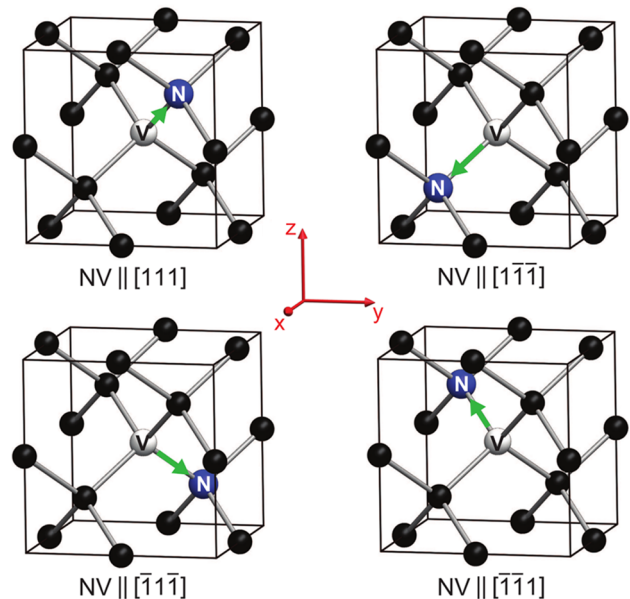


FIG. 1. Orientation of the NV centres within the diamond lattice. Four different orientations are depicted within the face-centred cubic Bravais lattice and their orientations are described according to Miller indices. In addition, there are four orientations (not shown), where the nitrogen atom and the vacancy change places. Figure adapted from Ref. [21]

### B. Quantum properties of NV centres and sensing applications

Over the past decades, research studying NV centres has provided us with an understanding of the underlying physics, based on empirical as well as ab initio results [5, 7]. Today, we can understand the properties of their magnetic moment, that are judged most important for future applications, in a simplified energy-level diagram, illustrated in Fig. 2. Note, here and in the following, we restrict ourselves to the negatively charged NV centres [5, 7]. The figure shows three electronic levels, two triplets and one singlet state. The ground state,  $|g\rangle$ , has a symmetry of  $^3A_2$ , the excited state,  $|e\rangle$ , has a symmetry of  $^3E$ , while the intermediate, metastable state,  $|s\rangle$ , actually involves two states with symmetries  $^1A_1$  and  $^1E$ . The so-called zero phonon line (ZPL), the main optical transition with a lifetime of about 10 to 30 ns [5], couples  $|g\rangle$  with  $|e\rangle$  and has a wavelength of  $\lambda_{ZPL} \simeq 637$  nm. Typically it is excited with  $\lambda_{exc} \simeq 532$  nm, while it can be excited in a broad band below. However, the fluorescence ranges also over a broad range and only a few percent of the photons are emitted into the ZPL; the major part emits into vibrational sidebands in the range of 630 to 800 nm [5, 7]. Non-radiative decay to  $|s\rangle$  can also occur, which, in turn, has a lifetime of about 250 ns. The fraction of radiative decay from  $|e\rangle$  depends on the spin state, as illustrated in Fig. 2 and this leads to a temporary optical contrast of about 30% between the

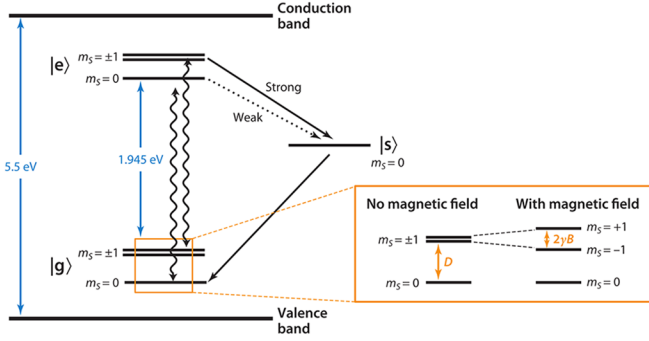


FIG. 2. Simplified energy level diagram of  $\text{NV}^-$  (not to scale). The electronic ground and excited, triplet states are labelled  $|g\rangle$  and  $|e\rangle$ , respectively, while an effective, singlet state is marked  $|s\rangle$ ; sub levels are labelled according to their spin quantum numbers  $m_s$ . Dipole allowed transitions are illustrated with wiggly arrows and other decay channels via are shown with straight arrows. Inset illustrates the Zeeman effect of the ground state manifold that allows for magnetic field sensing. The ground state manifold can be controlled using microwave radiation at around  $D \simeq 2\pi \times 2870$  MHz. Figure adapted from Ref. [7]

states  $|g, m_s = 0\rangle$  (bright state) and  $|g, m_s = \pm 1\rangle$  (dark state) when probing with the excitation light; this effect can be used for state detection/discrimination. After many scattering events the decay via  $|s\rangle$  pumps population into  $|g, m_s = 0\rangle$  and this can be used as state preparation. Ground-state manipulation can be achieved by microwave radiation near  $\omega_{\text{mw}} = 2\pi \times 2870$  MHz (for zero external magnetic field,  $B \simeq 0$ ) coupling  $|g, m_s = 0\rangle$  and  $|g, m_s = \pm 1\rangle$ . For  $B > 0$ , the two degenerate states  $|g, m_s = +1\rangle$  and  $|g, m_s = -1\rangle$  split according to the Zeeman effect  $\Delta E_{\text{Zeeman}} = \gamma m_s B$ , where  $\gamma \simeq 2$  denotes the electron gyromagnetic ratio. Typical experimental setups [5, 7] include a confocal microscope for application of excitation light and detection of fluorescence light. Further, the experimental setup includes a microwave sender, commonly, connected to a (micro-strip) transmission line that is brought into close proximity to the NV centre. For some experiments, it suffices to hold nanodiamonds on a glass slide under ambient conditions. The most effective sensing protocols would employ pulsed sequences, where an initial pulse of the excitation light prepares the bright state, followed by customised state manipulation pulses of microwave radiation, and concluded with a short pulse of the excitation light for state detection. Those customised state manipulation pulses are typically inspired by original work on nuclear magnetic resonance and atomic clocks [9]. For typical experiments on NV centres, the total protocol duration is limited by decoherence effects of the ground state manifold. At room temperature the dominating effect is spin-lattice relaxation, which happens on a time scale of a few milliseconds [5, 7]. Using such pulsed sequences, it has been demonstrated that NV centres can detect static magnetic fields [11–13] with a sensitivity of better than

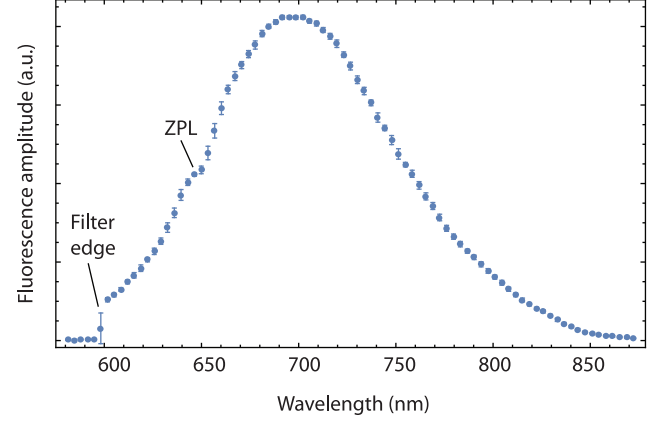


FIG. 3. Fluorescence spectrum of NV centres in micro-sized diamonds at room temperature. Laser light at 519 nm continuously excites fluorescence of the centres in the diamond. The spectrum is dominated by the vibrational band of the lattice. The zero phonon line (ZPL) at  $\simeq 640$  nm of the negative NV centres is indicated. The sharp edge at  $\simeq 600$  nm, results from an optical high-pass filter that is used to reduce scattered light from the excitation laser.

$0.36 \mu\text{T}/\sqrt{\text{Hz}}$  based on the above discussed Zeeman effect. Moreover, employing other effects that tune the details of the spin properties, it has been shown, e.g., to detect static electric fields [14] with a sensitivity of  $5.8 \text{ kV/cm}/\sqrt{\text{Hz}}$ , temperature [15] with  $0.1 \text{ K}/\sqrt{\text{Hz}}$ , and pressure [16] with  $0.6 \text{ MPa}/\sqrt{\text{Hz}}$  with single NV centres.

### C. NV fluorescence and optically detected magnetic resonances

In this lab course, we are using continuous measurement sequences that are sufficient for our purposes and require less complex data acquisition systems. But, they are less sensitive since they do not rely on coherence effects. In order to identify diamonds with negative NV centres, first of all we need to pick diamonds that emit red light when continuously excited with green laser light. In Figure 3, we show an example of a fluorescence spectrum recorded with our lab course setup. Here, we find a ZPL at about 640 nm that identifies the presence of negative centres.

In addition, we can optically detect magnetic resonances of such centres. Again, we continuously apply laser excitation, but combined with microwave radiation at about  $2\pi \times 2.85$  GHz, and record the fluorescence with a photo detector. In this way we can monitor variable magnetic fields. Typical results of two of such measurements are shown in Fig. 4. Data is depicted in comparison to a corresponding model fit (solid lines). The top graph depicts a single resonance for an external magnetic field close to zero, while the bottom illustrates multiple resonances at an field strength of  $B \simeq 23$  G. More than two lines are the result of multiple defects that are aligned

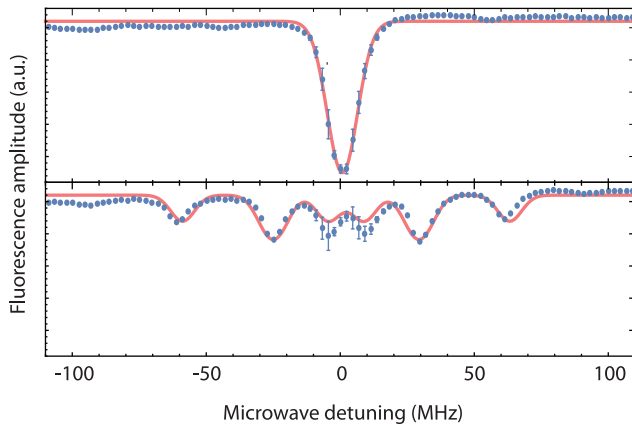


FIG. 4. Optically detected magnetic resonances for variable external magnetic field. Data points are the result of an average of 64 repetitions and solid lines depict model fits to the data. (Top) Microwave spectrum for an external magnetic field strength of  $B \simeq 0$  (only stray magnetic fields are present). (Bottom) Spectrum for  $B \simeq 25$  G, the orientation of the diamond lattice with respect to the external magnetic field axis can be estimated from the observed Zeeman splitting and due to the fact that multiple NV centres are observed simultaneously.

in multiple directions, i.e., in the studied micro diamond we find more than one NV centre. From the line splittings, we can determine the lattice orientation of a mono crystalline diamond with respect to the direction of the external field. However, this estimation may require to subsequently record spectra with magnetic fields from various directions.

## II. EXPERIMENTAL SETUP

During the lab course, students work with an experimental setup that they are required to characterise and optimise, cp Sec. III B for details. In the following, we give a brief overview of the available equipment and a description of one possible realisation of such a final setup used for the investigation of NVs in diamonds, see Sec. II C. For their studies, students need to employ various optical, microwave, and other electronic components. In particular, calibration setups require individual rearrangements of the components and students are free to combine available equipment. For a list of the most important elements, we refer to Sec. IV

### A. Laser source and optical components

As a light source, we utilise a diode laser with a maximum output power of 100 mW and a wavelength of about 519 nm. This source is classified as a Class-3b system, and it is required that users wear appropriate laser safety goggles when operating the laser. The turn-key system

can be controlled via a software interface and is fibre coupled. A tune able fibre coupler is used to optimise the spatial characteristics of the laser beam and several additional optical elements, e.g., aspheric lenses, beam splitters, dichroic mirrors, and filters, are available for the experiments. We deploy a compact CMOS camera to spatially resolve individual micro-sized diamonds. To study characteristics of the fluorescence light of NV centres in these diamond samples, we install a compact spectrometer and an avalanche photo diode (APD).

### B. Electronic and microwave equipment

For the measurements of the optically detected magnetic resonances, of the ground-state manifold we make use of a chain of microwave components. The microwave signal is taken from the tracking generator of a spectrum analyser. In turn, the input of that same analyser can be employed to characterise all other microwave components. Note, the maximum input power of the spectrum analyser is 30 dBm, i.e., do not connect the output of the main amplifier to it! These components are, e.g., an input coupler, attenuators, and a high-power amplifier with an maximum output of 16 W. We designed and our electronics workshop manufactured a micro-strip line where we can place the diamonds and send in the microwave signal for recording the magnetic resonances. Further, in each lab course students may decide to build a low-pass filter using their choice of resistors and capacitors to filter noise picked up by the APD signal. For amplifying the fluorescence recorded by the APD, we can use an audio amplifier with variable gain.

### C. Apparatus for NV centre spectroscopy

One possible realisation of a final apparatus that needs to be set up by the students for the spectroscopy of individual diamonds is depicted in Fig. 5. It can be used for the measurements described in Sec. III C and can give results that are comparable to the descriptions in Sec. I C. It combines diamonds placed on the micro-strip PCB board that is fed by the amplified output of the tracking generator of the spectrum analyser. In this way, up to 42 dBm of microwave power in the range of  $\omega_{mw}/(2\pi) \simeq 2.0$  GHz to 3.0 GHz can be applied for the measurements. Note, the temperature of the PCB board is monitored and when it's temperature reaches about 40 °C, the source needs to be turned off. Further, the laser beam is focused onto a specific diamond for characterisation and, ideally, to excite NV fluorescence. The fluorescence light is collected by the aspheric lens and guided toward the detection region, where it can be recorded by the CMOS camera, the spectrometer, and the APD. Corresponding signals can be monitored on the PC or the oscilloscope. Depending on the type of measurement, optical and electronic filters or amplifiers



the following, we give a list of examples of these figure of merits:

- Size and shape of the diamonds,
- Fluorescence spectra,
- Microwave spectrum with approx. zero external magnetic field,
- Number of NV centre orientations within the monocrystal,
- Orientation of the diamond lattice in the laboratory frame.

Students choose appropriate measurement sequences to determine these values. Finally, they can record sequences with variable magnetic field strengths using their *favourite* diamond as the field probe and determine the corresponding magnetic field sensitivity.

#### IV. APPENDIX

In Table I, we list all available equipment and corresponding manuals are stored on the lab computer or can be found online (follow link).

- 
- [1] I. Aharonovich, A. D. Greentree, and S. Prawer, *Nat. Photonics* **5**, 397 (2011).
  - [2] T. D. Ladd, F. Jelezko, R. Laflamme, Y. Nakamura, C. Monroe, and J. L. O'Brien, *Nature* **464**, 45 (2010).
  - [3] V. N. Mochalin, O. Shenderova, D. Ho, and Y. Gogotsi, *Nat. Nanotechnol.* **7**, 11 (2011).
  - [4] I. Aharonovich, S. Castelletto, D. A. Simpson, C.-H. Su, A. D. Greentree, and S. Prawer, *Reports Prog. Phys.* **74**, 076501 (2011).
  - [5] M. W. Doherty, N. B. Manson, P. Delaney, F. Jelezko, J. Wrachtrup, and L. C. Hollenberg, *Phys. Rep.* **528**, 1 (2013).
  - [6] I. M. Georgescu, S. Ashhab, and F. Nori, *Rev. Mod. Phys.* **86**, 153 (2014).
  - [7] R. Schirhagl, K. Chang, M. Loretz, and C. L. Degen, *Annu. Rev. Phys. Chem.* **65**, 83 (2014).
  - [8] J. Wrachtrup, *Ger. Res.* **37**, 20 (2015).
  - [9] D. J. Wineland, *Rev. Mod. Phys.* **85**, 1103 (2013).
  - [10] D. Leibfried, R. Blatt, C. Monroe, and D. Wineland, *Rev. Mod. Phys.* **75**, 281 (2003).
  - [11] G. Balasubramanian, I. Y. Chan, R. Kolesov, M. Al-Hmoud, J. Tisler, C. Shin, C. Kim, A. Wojcik, P. R. Hemmer, A. Krueger, T. Hanke, A. Leitenstorfer, R. Bratschitsch, F. Jelezko, and J. Wrachtrup, *Nature* **455**, 648 (2008).
  - [12] J. R. Maze, P. L. Stanwix, J. S. Hodges, S. Hong, J. M. Taylor, P. Cappellaro, L. Jiang, M. V. G. Dutt, E. Togan, A. S. Zibrov, A. Yacoby, R. L. Walsworth, and M. D. Lukin, *Nature* **455**, 644 (2008).
  - [13] J. M. Taylor, P. Cappellaro, L. Childress, L. Jiang, D. Budker, P. R. Hemmer, A. Yacoby, R. Walsworth, and M. D. Lukin, *Nat. Phys.* **4**, 810 (2008).
  - [14] F. Dolde, H. Fedder, M. W. Doherty, T. Nöbauer, F. Rempp, G. Balasubramanian, T. Wolf, F. Reinhard, L. C. L. Hollenberg, F. Jelezko, and J. Wrachtrup, *Nat. Phys.* **7**, 459 (2011).
  - [15] D. M. Toyli, D. J. Christle, A. Alkauskas, B. B. Buckley, C. G. Van de Walle, and D. D. Awschalom, *Phys. Rev. X* **2**, 031001 (2012).
  - [16] M. W. Doherty, V. V. Struzhkin, D. A. Simpson, L. P. McGuinness, Y. Meng, A. Stacey, T. J. Karle, R. J. Hemley, N. B. Manson, L. C. Hollenberg, and S. Prawer, *Phys. Rev. Lett.* **112**, 047601 (2014).
  - [17] O. Arcizet, V. Jacques, A. Siria, P. Poncharal, P. Vincent, and S. Seidelin, *Nat. Phys.* **7**, 879 (2011).
  - [18] P. Maletinsky, S. Hong, M. S. Grinolds, B. Hausmann, M. D. Lukin, R. L. Walsworth, M. Loncar, and A. Yacoby, *Nat. Nanotechnol.* **7**, 320 (2012).
  - [19] V. R. Horowitz, B. J. Alemán, D. J. Christle, A. N. Cleland, and D. D. Awschalom, *Proc. Natl. Acad. Sci.* **109**, 13493 (2012).
  - [20] O. M. Maragò, P. H. Jones, P. G. Gucciardi, G. Volpe, and A. C. Ferrari, *Nat. Nanotechnol.* **8**, 807 (2013).
  - [21] L. M. Pham, *Magnetic field sensing with nitrogen-vacancy color centers in diamond*, Tech. Rep. (DTIC Document, 2013).



TABLE I. List of available equipment

Description	Vendor	Part No.	Specifications
Laser	Toptica	IBeam-SMART-515-S	$< 100 \text{ mW}$ at $\simeq 519 \text{ nm}$
Compact CCD Spectrometers	Thorlabs	CCS175/M	see: <a href="#">link</a>
CMOS Camera	Thorlabs	DCC1545M	see: <a href="#">link</a>
Avalanche photo diode	Thorlabs	APD430A2/M	see: <a href="#">link</a>
Spectrum analyser	RIGOL	DSA 1030	$< 10 \text{ dBm}$ from $9 \text{ kHz}$ to $3.0 \text{ GHz}$
Oscilloscope	RIGOL		
Microwave amplifier	Mini Circuits	ZHL-16W-43-S+	see <a href="#">link</a>
Audio amplifier			
Aspheric lense	Thorlabs		
Plano-convex lense	Thorlabs		
Dichroic Mirror	Thorlabs	DMLP550	
$2\times$ Optical longpass filter	Thorlabs	FELH0600	
Optical band-pass filter	Thorlabs		
Optical beam splitter 50:50	Thorlabs		
Optical beam splitter 90:10	Thorlabs		
Coupler for microwaves	Mini-Circuits	ZADC-10-63-S+	